Channel Capacity Experiment of a Polarization Controlled MIMO Antenna for Wearable Applications

Kun Li, Kazuhiro Honda, and Koichi Ogawa
Graduate School of Engineering, Toyama University
3190 Gofuku, Toyama-shi, Toyama 930-8555, Japan

Abstract— This paper presents a preliminary experiment for evaluating the channel capacity of a 2×2 polarization-controlled MIMO antenna that takes the variation of the radio wave propagation environment and the antenna inclination angle into consideration simultaneously. Firstly, the radiation pattern of a 2×2 polarization-controlled MIMO antenna was measured in an anechoic chamber. Then, the MIMO channel capacity measurement has been carried out under different use scenarios using an OTA apparatus. From an agreement between the measured data and analytical results, the effectiveness of the proposed antenna was confirmed.

1. INTRODUCTION

A Small Cell era is coming for realizing ultra-high-capacity mobile communications using multiple-input multiple-output (MIMO) technique as a result of the development of LTE, LTE-Advanced and Beyond 4G cellular systems. Since mobile terminals are used close to base stations in the urban area, the cross polarization power ratio (XPR) will increase and vary significantly. Further, a polarization mismatch will also occur easily due to the variation in the inclination angle of an antenna caused by the operator's dynamic motions. In order to solve such difficulties, we proposed a 3-axis weighted-polarization active antenna that can realize a large-capacity transmission in wearable radio applications in an analytical way [1].

For the purpose of confirming the validity of the proposed antenna, this paper presents a preliminary experiment for evaluating the channel capacity of a polarization-controlled MIMO antenna. Firstly, the configuration of the proposed 3-axis weighted-polarization active antenna is introduced. Then, the radiation pattern of the 2×2 polarization-controlled MIMO antenna was measured in an anechoic chamber. Finally, the MIMO channel capacity measurement has been carried out under different use scenarios using an OTA apparatus. From an agreement between the measured data and analytical outcomes, the effectiveness of the proposed antenna is verified, demonstrating that the proposed antenna is useful for realizing the gigabit mobile communications in forthcoming high-speed and wearable mobile applications.

2. 3-AXIS WEIGHTED-POLARIZATION ACTIVE ANTENNA

Figure 1 shows the configuration of the 3-axis weighted-polarization active antenna [1]. The proposed antenna is comprised of three orthogonal dipole antennas (A_x, A_y, A_z). When the antenna is rotated by the operation of a user, two of the three dipole antennas are selected using two switches (SW_1, SW_2). The received signals (vertical polarization s_V and horizontal polarization s_H) from two selected antennas are combined using the weight function created based on the variation of XPR and the variation due to the antenna inclination angle (α). As shown in Fig. 1, the received signals (s_V, s_H) are multiplied by the weight functions (W_V, W_H). Consequently, the signal at an output port (a) of the proposed antenna is expressed by the following equation:

$$a = W_V s_V + W_H s_H \tag{1}$$

where the weight functions (W_V, W_H) are calculated by the allotment of signals under the XPR, and are given by:

$$W_V = \sqrt{\frac{XPR}{1+XPR}}, \tag{2}$$

$$W_H = \sqrt{\frac{1}{1+XPR}}, \tag{3}$$

Figure 2 shows the situation that the proposed antenna (see Fig. 1) is mounted on a tablet handset. The holding angle α of the tablet handset is changed by an operator, which will cause the

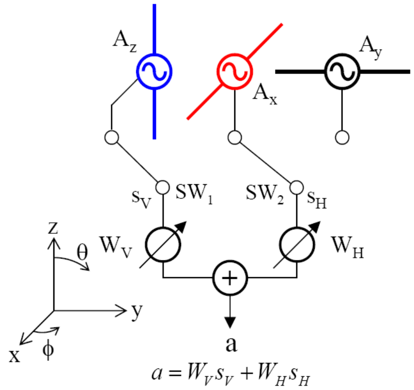

Figure 1: 3-axis weighted-polarization active antenna.

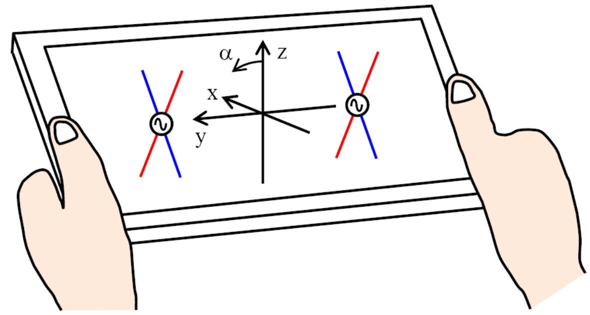

Figure 2: Holding angle α in a tablet handset.

variation of antenna polarization. Therefore, the weight functions (2), (3) are not appropriate for the situation in Fig. 2 where the antenna is inclined. Thus, the following equations are presented:

$$a = W'_V s_V + W'_H s_H e^{j\frac{\pi}{2}} \quad (4)$$
$$W'_V = W_V \left|\cos\alpha\right| + W_H \left|\sin\alpha\right| \quad (5)$$
$$W'_H = W_V \left|\sin\alpha\right| + W_H \left|\cos\alpha\right|, \quad (6)$$

where the weight functions (W'_V, W'_H) are provided considering both the weight functions defined by the Equations (2), (3) (W_V, W_H) and the variation of holding angle (α). A quadrature phase shift appearing in the last term in Equation (4) is needed because there is a cancellation between the vertically or horizontally polarized component of the vertical antenna and that of the horizontal antenna when the proposed antenna is inclined, as shown in Fig. 2. As described in this manner, the Equation (5), (6) present a method of signal combination in consideration of the antenna polarization characteristics caused by the variation of holding angle.

In order to confirm the validity of the proposed method, a preliminary measurement using a 2×2 polarization-controlled MIMO antenna has been carried out, as will be introduced hereafter.

3. RADIATION PATTERN

Firstly, the radiation pattern of a 2×2 polarization-controlled MIMO antenna was measured in an anechoic chamber. Fig. 3 shows the structure of the 2×2 MIMO array antenna comprised of two dipole antennas. The two orthogonal half-wavelength dipole antennas were arranged as a MIMO array antenna in the y-direction. The space between the two array elements was set to 18 cm. The array antenna is attached to a jig that can change the antenna inclination angle as we need. The frequency for the design is 950 MHz.

The attenuator was used to represent the weight function mentioned in Section 2. Table 1 shows an example of the setup of the attenuators A_v and A_H indicate the actual attenuation in the attenuators while W'_v and W'_H indicate the analytical weight functions illustrated by the

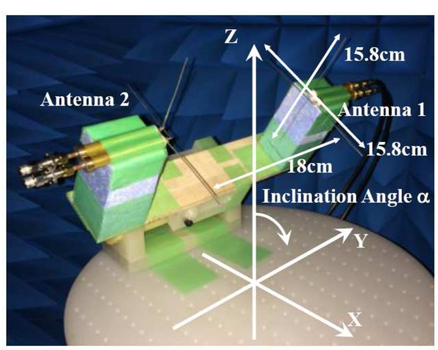

Figure 3: Configuration of the 2×2 MIMO antenna.

Table 1: Setup of attenuators.

XPR [dB]	α [deg]	A_V	A_H	$\frac{A_V}{A_H}$	W'_V	W'_H	$\frac{W'_V}{W'_H}$
0	0	1.00	1.00	1.0	0.50	0.50	1.0
10	0	1.00	0.10	10	0.90	0.10	10
20	0	1.00	0.01	100	0.99	0.01	100
20	30	1.00	0.42	2.4	0.71	0.29	2.4
20	45	1.00	1.00	1.0	0.50	0.50	1.0

Equations (5) and (6). The power ratio of A_v and A_H was adjusted to set the ratio of W'_v and W'_H for realizing the proposed polarization-controlled method in different use scenarios For example, when the XPR is set to 0 dB and α is fixed at 0 degree, the weight functions W'_v and W'_H have the same value because there is no polarization distribution in this situation. Therefore, the attenuators that are connected to the vertical and horizontal antennas will be set to unity (0 dB) for both cases. However, when the XPR is set to 20 dB and α is fixed at 30 degree, a polarization mismatch will occur so that we set the values of the attenuators to be $A_v = 1$ (0 dB) and $A_H = 0.42$ (-3.77 dB). This allows the ratio of A_v and A_H to be 2.4 (3.77 dB) to achieve the same power ratio as in the theoretical weight functions W'_v and W'_H. The method of setting the attenuators in the antenna side will also be applied to the measurement of MIMO channel capacity, as will be presented in Section 4.

Figures 4 and 5 present the measured and analytical results of the radiation patterns for the polarization controlled 2×2 MIMO antenna in the horizontal plane. The XPR was set to two values: XPR = 0 dB and 20 dB, as shown by Figs. 4(a) and (b), respectively. In Fig. 4, the antenna inclination angle (α) was fixed at 0 degree while, in Fig. 5, α was set to 30 degrees. The blue lines indicate the E_θ while the red lines indicate the E_ϕ, which denote the electric field directivity of the antenna element for the θ and ϕ components, respectively.

As shown by Figs. 4(a) and (b), when α was fixed at 0 degree, with an increase in XPR from 0 to

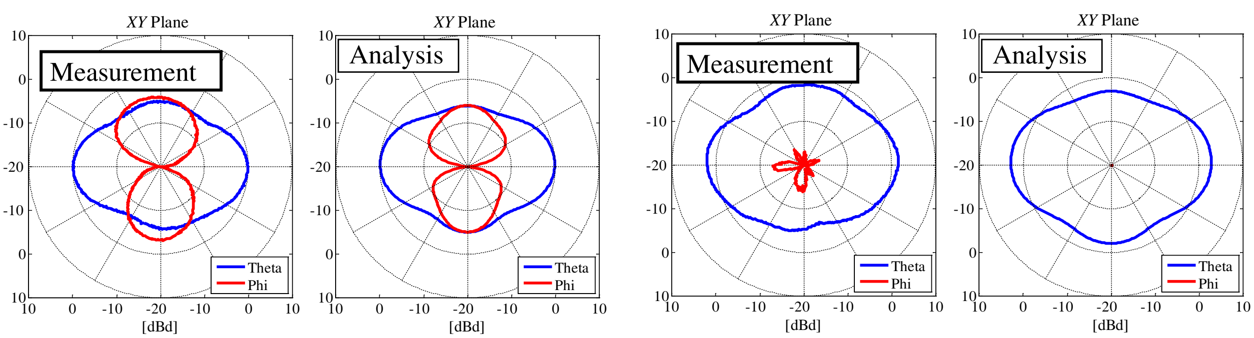

(a) XPR=0 dB (b) XPR=20 dB

Figure 4: Measured and analyzed results of the radiation pattern with different XPRs ($\alpha = 0$ deg).

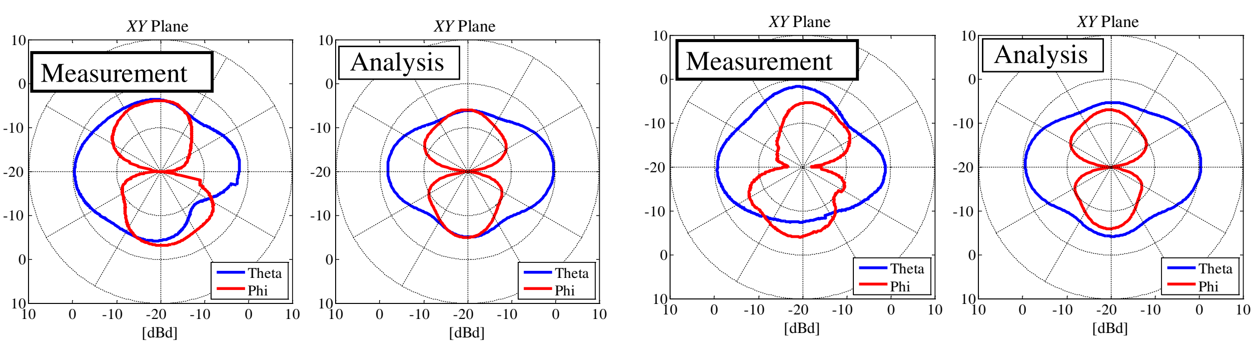

(a) XPR=0 dB (b) XPR=20 dB

Figure 5: Measured and analyzed results of the radiation pattern with different XPRs ($\alpha = 30$ deg).

20 dB, the vertically polarized component in the radiation pattern is large whereas the horizontally polarized component disappears. This is a desirable characteristic for an antenna operated in a radio propagation environment with a large XPR of 20 dB because a strong vertical polarization appears in that environment. This fact indicates that the weight function works well according to the change of the XPR.

In Fig. 4(a) and Fig. 5(a), when the XPR was 0 dB, similar radiation patterns can be observed even when α was changed from 0 to 30 degrees. This characteristic is also desirable for an antenna in a propagation environment with XPR = 0 dB because almost the same radiation intensity of E_θ and E_ϕ, as shown in Figs. 4(a) and 5(a), means that an optimum combination of θ and ϕ polarized incident waves can be achieved due to the identical amplitude of the two polarized incident waves. This particular nature of the proposed antenna is originated from the fact that the weight function W'_v and W'_H derived from Equations (5) and (6) are unchanged when XPR = 0 dB, leading to a similar radiation pattern regardless of the antenna inclination angle α. Consequently, our intention to design the proposed antenna is successfully satisfied.

However, when we compare Fig. 4(b) with Fig. 5(b), where XPR = 20 dB, a large E_ϕ component can be seen in Fig. 5(b) in the case of $\alpha = 30$ deg. This is an undesirable characteristic because a ϕ-polarized incident wave is not dominant when XPR = 20 dB. This observation can be attributed to the fact that only the amplitude-controlled operation was considered in the proposed weighting method, so that an undesired polarization component generated by an increased α cannot be suppressed sufficiently. This viewpoint can be supported by Fig. 8, where there is a slight degradation in the MIMO channel capacity when α is 30 degrees and XPR is 20 dB, as indicated by the position Q_1. Despite this drawback, the channel capacity still maintains at a high level compared with the position Q_2 where α is 0 degree, indicating that the effectiveness of proposed weight function according to the simultaneous variation of the XPR and α.

4. MIMO CHANNEL CAPACITY

After the weight function was confirmed by the measurement of the radiation patterns, the MIMO channel capacity of a 2 × 2 polarization-controlled MIMO antenna was measured by an OTA apparatus.

The spatial fading emulator for the MIMO-OTA testing is shown in Fig. 6(a) The 2 × 2 MIMO antenna mentioned in Section 3 was set at the center of the fading emulator. The fading emulator has 7 scattering units located at equal intervals around a circle with 2.4 m in diameter surrounded by electromagnetic absorbers Each unit is comprised of two orthogonal half-wavelength dipole antennas to create the cross-polarized fading signals Fig. 6(b) shows the microwave circuit that controls the signals radiated from the scatterers. The circuit is comprised of 14 sets of phase shifters and attenuators, which is divided by two groups of vertical and horizontal polarization components for creating the XPR as needed Using this OTA apparatus, the MIMO channel capacity of a 2 × 2 polarization-controlled MIMO antenna under different use scenarios (XPR and α) was measured.

Figure 7 shows the measured results of 2 × 2 MIMO channel capacity as a function of the XPR when the antenna inclination angle (α) was fixed at 0 degree. Fig. 8 shows the measured results of 2 × 2 MIMO channel capacity as a function of the antenna inclination angle (α) when the XPR was fixed at 20 dB. The SNR of incident wave was set to 30 dB. In Figs. 7 and 8, the black line shows

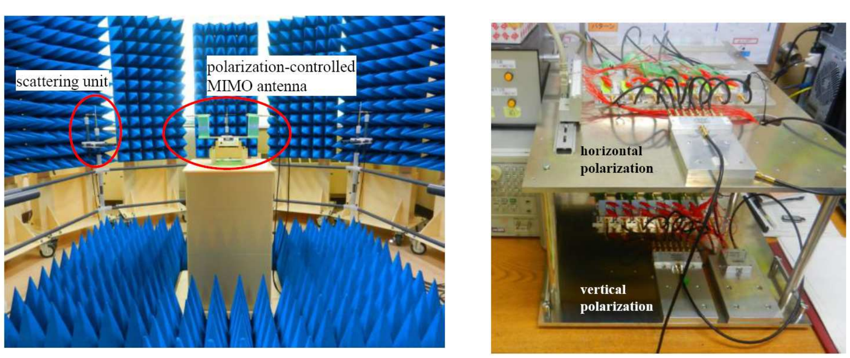

(a) Spatial fading emulator (b) Control circuit

Figure 6: Spatial fading emulator and control circuit.

the measured results obtained from the fading emulator while the red line indicates the analytical outcome calculated by the Monte Carlo simulation [2].

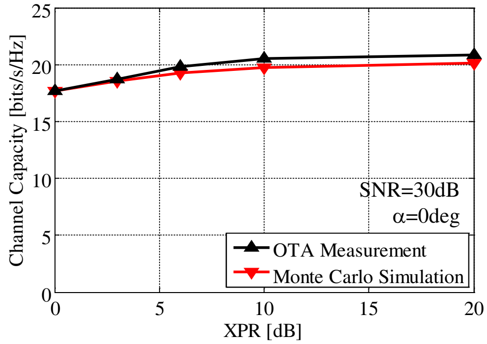

Figure 7: MIMO channel capacity vs. XPR.

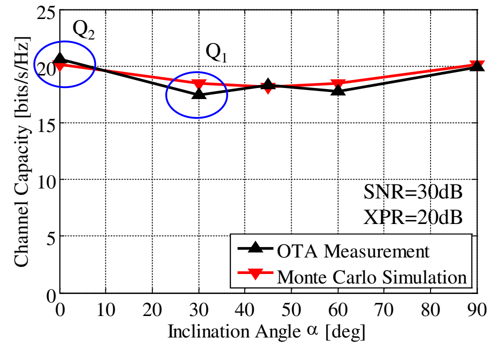

Figure 8: MIMO channel capacity vs. inclination angle α.

As can be seen in Fig. 7, in different propagation environments (XPR), the measured results agree well with the analytical outcome, indicating that a stable channel capacity can be observed. Therefore, in propagation environments where XPR is changed in a great extent a high level of channel capacity can be obtained and maintained using the proposed polarization-controlled antenna.

In Fig. 8, a good agreement between the measured results and the analytical outcome can be observed, indicating that in different antenna inclination angle (α), the same level of channel capacity can be obtained and maintained using the proposed antenna.

Therefore, the validity of the proposed weighted-polarization method is confirmed by the experiments for radiation pattern and MIMO channel capacity using the 2×2 polarization-controlled MIMO antenna.

5. CONCLUSION

This paper presents a preliminary experiment for evaluating the channel capacity of the proposed MIMO antenna. The measured radiation pattern and channel capacity of a 2×2 MIMO weighted-polarization antenna coincide well with the analytical results, indicating the effectiveness of the weight functions used in the propose antenna. The realization of gigabit mobile communications using the proposed antenna are anticipated in forthcoming high-speed and wearable cellular applications, and this will be addressed in our future works.

ACKNOWLEDGMENT

This work was supported in part by the SCOPE 2013 grant number 135005102.

REFERENCES

1. Honda, K., K. Li, and K. Ogawa, "An 8×8 MIMO 3-axis weighted polarization active antenna for wearable radio applications," *31th URSI General Assembly and Scientific Symposium*, Beijing, China, Aug. 2014, to be Presented.
2. Ogawa, K., H. Iwai, A. Yamamoto, and J. Takada, "Channel capacity of a handset MIMO antenna influenced by the effects of 3D angular spectrum, polarization, and operator, " *IEEE AP-S Intl. Symp. Digest*, 153–156, Jul. 2006.